CrossMark

# Decrement of coke from phenol hydroxylation on iron on zeolite beta by employing dealuminated support

Onsulang Sophiphun[1] · Dilek Demir[2] ·
Karin Föttinger[2] · Günther Rupprechter[2] ·
Sirinuch Loiha[3] · Arthit Neramittagapong[4] ·
Sanchai Prayoonpokarach[1] · Jatuporn Wittayakun[1]

**Abstract** An attempt to decrease coke formation from phenol hydroxylation on iron catalyst supported on zeolite beta (Fe/HBEA) was investigated. HBEA was dealuminated by refluxing in nitric acid. The dealumination removed all framework aluminum atoms and presumably generated hydroxyl nests of the tetrahedral vacant sites which were strongly acidic. An iron catalyst supported on dealuminated zeolite beta (Fe/D-BEA) was prepared by stirring the dealuminated HBEA in a solution of $Fe(NO_3)_2$. The obtained catalyst had an Fe loading 2.60 wt%. The Fe had an oxidation state $+3$ and tetrahedral coordination. After loading, the zeolite structure was slightly contracted by the insertion of Fe ions into the vacant sites and calcination. The strong acid sites on D-BEA were suppressed. When Fe/D-BEA was tested in phenol hydroxylation, a steady conversion around 56 % was reached in 6 min. Catechol and hydroquinone were the major products with the mole ratio 2:1. However, cokes were still observed. The type of cokes from Fe/D-BEA was similar to those from Fe/HBEA but the amount from Fe/D-BEA was lower. Thus, the product yields from Fe/D-BEA were higher.

**Keywords** Zeolite beta · BEA · Dealumination · Iron · Phenol hydroxylation

✉ Jatuporn Wittayakun
jatuporn@sut.ac.th

1   School of Chemistry, Institute of Science, Suranaree University of Technology, Nakhon Ratchasima 30000, Thailand

2   Institute of Materials Chemistry, Technische Universität Wien, 1060 Vienna, Austria

3   Department of Chemistry, Faculty of Science, Khon Kaen University, Khon Kaen 40002, Thailand

4   Department of Chemical Engineering, Faculty of Engineering, Khon Kaen University, Khon Kaen 40002, Thailand

## Introduction

Recently, iron (Fe) was loaded on zeolite beta in proton form (HBEA) by various methods and tested in phenol hydroxylation [1]. The Fe/HBEA prepared from ion exchange method was the most active catalyst but after the catalytic testing coke was observed. The goal of this work was to decrease coke by employing a catalyst with lower acidity. Thus, HBEA was dealuminated by nitric acid before the addition of Fe. The obtained catalyst was expected to lessen the coke and increase the product yield. The activity of HBEA alone (Si/Al = 12.5 and 75) in phenol hydroxylation was reported by Atoguchi et al. [2]. At 100 °C in the presence of $H_2SO_4$, they found that the HBEA with less Al content gave the higher product yield.

Substitution of Si in a zeolite framework by Al generates a negative charge, which requires a charge balancing cation. When the cation is proton, a Brønsted acid site is obtained [3]. Moreover, the calcination of a zeolite in proton form leads to dehydroxylation, which generates tricoordinated $Al^{3+}$, a Lewis acid site [4, 5]. Thus, the number of acid sites depends on the Si/Al ratio. The acid sites of the zeolite can interact with hydrocarbon intermediates from the reactions of organic compounds leading to the formation of cokes or tarry compounds [6, 7]. A simple method to decrease acid sites is dealumination by treating the zeolite with a mineral acid such as nitric or hydrochloric acid [8–10]. The acid removes both framework and extraframework aluminum.

In this work, HBEA was dealuminated by nitric acid, loaded with Fe and tested in phenol hydroxylation. The properties of the dealuminated zeolite and the Fe catalyst was investigated by X-ray fluorescence (XRF), X-ray diffraction (XRD), X-ray absorption near edge structure (XANES) spectroscopy, diffuse reflectance ultraviolet–visible (DR-UV–vis) spectroscopy and ammonia temperature-programmed desorption ($NH_3$-TPD). The spent catalyst were analyzed by temperature-programmed oxidation (TPO) to compare the amount of cokes.

## Experimental

### Sample preparation

With a procedure modified from the literature [8], 15 g of HBEA (Süd-Chemie AG, Si/Al = 17) was dealuminated with nitric acid (6.5 M, 150 mL) at 80 °C under stirring (1400 rpm) for 30 min. Then, the solid was separated by centrifugation, washed with DI water and dried overnight at 100 °C. The obtained solid was named D-BEA.

The catalyst Fe/D-BEA was prepared by stirring 3 g of D-BEA in an aqueous solution of $Fe(NO_3)_3$ ($1.8 \times 10^{-2}$ M, 150 mL) at room temperature for 24 h [1]. The solid was separated by centrifugation, washed with DI water, dried and calcined at 450 °C for 3 h.

### Catalyst characterization

Elemental composition of D-BEA and Fe/D-BEA was obtained by energy dispersive XRF (Horiba Scientific XGT-5200). Powder XRD patterns were

recorded on a Bruker AXS D5005 diffractometer using nickel filtered Cu $K_\alpha$ radiation. The acidity of HBEA, D-BEA and Fe/D-BEA was analyzed by $NH_3$-TPD using a BELCAT analyser. Each sample (50 mg) was pretreated at 500 °C for 1 h in He stream with a total flow rate of 50 mL/min. After cooling down to 100 °C, the sample was exposed to 35 % $NH_3$/He for 1 h and purged by He for 1 h. Then, desorption was performed by heating the sample to 700 °C. Signals of desorbed $NH_3$ were recorded by a thermal conductivity detector (TCD).

The oxidation state of Fe in Fe/D-BEA was determined by XANES at the XAS Beamline 5.2 (SUT-NANOTEC-SLRI) at the Synchrotron Light Research Institute, Thailand. The storage ring was operated with the electron energy 1.2 GeV. The electron current during the measurement was between 90 and 140 mA. Double Ge (2 2 0) crystals were used as synchrotron X-ray monochromators. The photon energy was calibrated using a standard Fe foil. The sample was analyzed from 7100 to 7190 eV with a step of 0.2 eV. Moreover, the coordination of Fe was analyzed by DR-UV–vis spectroscopy on a Perkin Elmer, Lambda 750 in the range of 190–700 nm with a resolution of 3 nm. $BaSO_4$ was used as a non-absorbing standard.

## Catalytic testing in phenol hydroxylation

The catalyst was tested in phenol hydroxylation in a batch-type reactor as described in the previous work [1]. The products were analyzed by a gas chromatograph (Shimadzu 14A series) equipped with an ID-BP1 coated capillary column and a flame ionization detector. The phenol conversion was calculated by Eq. 1 and the product yield was calculated by Eq. 2.

$$\text{Phenol conversion (\%)} = \left( \frac{\text{Initial mole of phenol} - \text{final mole of phenol}}{\text{Initial mole of phenol}} \right) \times 100 \tag{1}$$

$$\text{Product yield (\%)} = \left( \frac{\text{Mole of target product}}{\text{Initial mole of phenol} - \text{final mole of phenol}} \right) \times 100 \tag{2}$$

## Characterization of spent catalysts by TPO

After being tested in phenol hydroxylation for 45 min, the Fe/D-BEA catalyst was separated by centrifugation, washed with distilled water and air-dried at room temperature. The spent catalyst (22 mg) was added to an alumina pan and analyzed by a thermal analyzer, NETZSCH STA 449 F3 Jupiter® connected with a mass spectrometer and heated from 25 to 800 °C in 3 % $O_2$ in Ar stream with the flow rate of 20 mL/min. The sample weight loss and the MS signals of produced $CO_2$ ($m/z = 44$) were recorded. For comparison, the spent Fe/HBEA from the previous work was analyzed with the similar procedure.

# Results and discussion

## Characterization

The Si/Al atomic ratio of HBEA determined by XRF was 17.5. After dealumination, Al was not detected indicating a complete removal. For Fe/D-BEA, the Fe loading was 2.60 wt% and the Si/Fe ratio was 31.7. The Si/Fe ratio was lower than Si/Al ratio implying that vacant sites, previously occupied by Al, were partially filled by Fe.

XRD patterns for D-BEA and Fe/D-BEA are compared with that of HBEA in Fig. 1. From HBEA, the main peaks were observed at 7.71° and 22.50°, which are characteristic of the BEA structure. From D-BEA, the two main peaks were still observed indicating that the zeolite structure was not destroyed by dealumination. However, the diffraction peaks of D-BEA were observed at 7.72° and 22.64°. The shift to higher angles after dealumination indicated a contraction of the BEA lattice. A similar phenomenon was also reported in the literature [11, 12]. After Fe loading and calcination, the peaks from Fe/D-BEA were observed at 7.82° and 22.70°. The further shift suggested a further contraction of the structure. This observation was in contrary to the report by Dzwigaj and Che [11] and Gurgul et al. [12]. After adding Co and Fe to dealuminated HBEA, they observed the shift of XRD peaks to lower angles implying the insertion of metal cations to the vacant tetrahedral sites formerly occupied by Al. Thus, it was necessary to determine the coordination nature of Fe.

The XANES spectra of Fe/D-BEA catalysts are compared with those of $Fe_2O_3$ and $Fe(NO_3)_3 \cdot 9H_2O$ standards in Fig. 2a. The K-edge energy of Fe in Fe/D-BEA was 7126.51 eV, not significantly different from those of $Fe_2O_3$ and $Fe(NO_3)_3 \cdot 9H_2O$, which were 7125.47 and 7127.63 eV, respectively. The result indicated that the oxidation state of Fe in Fe/D-BEA was +3. The pre-edge corresponding to Fe with tetrahedral coordination [15, 16] was observed in the spectra of Fe/D-BEA.

Fig. 2b shows DR-UV–vis spectrum of Fe/D-BEA. The main absorption bands at 217 and 267 nm were assigned to charge transfer from oxygen to Fe(III) with tetrahedral coordination [12, 13]. This results confirmed that Fe was added to the vacant tetrahedral sites formerly occupied by Al(III). Thus, the main location of



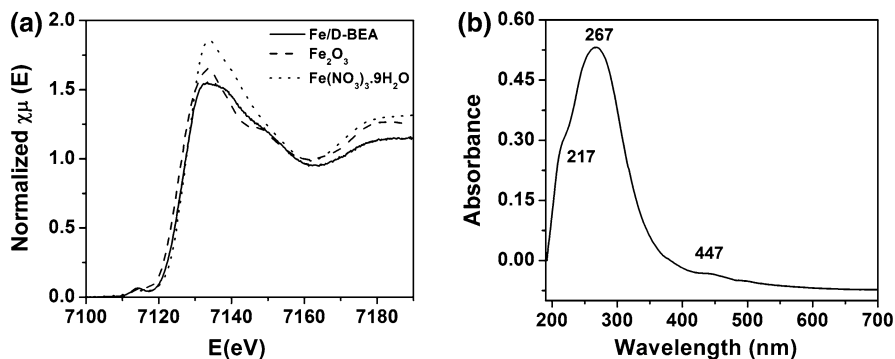Fig. 1 XRD patterns of HBEA, D-BEA and Fe/D-BEA
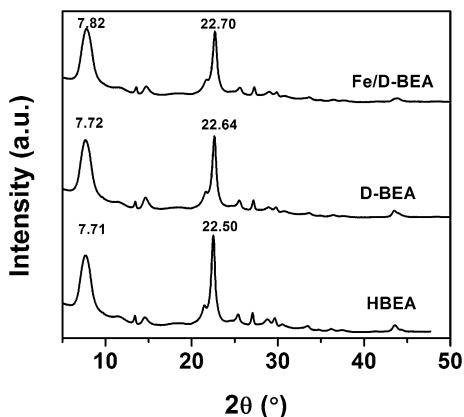
**Fig. 2** **a** DR-UV–vis spectrum of Fe/D-BEA and **b** XANES spectrum of Fe/D-BEA

Fe(III) was in the zeolite framework. In addition, a small band at around 447 nm was observed and attributed to charge transfer from oxygen to Fe(III) with octahedral coordination [12, 14]. The results indicated the presence of a small amount of extraframework $FeO_x$ oligomers on the zeolite [12].

$NH_3$-TPD profiles of HBEA, D-BEA and Fe/D-BEA are compared in Fig. 3. From HBEA, there were two desorption peaks at 160 and 456 °C. The peak at low temperature could be related to extraframework Al [17] or zeolite defects [18, 19]. The peak at high temperature corresponded to isolated silanol or hydroxyl nests in the zeolite structure which are Brønsted acid sites [8]. From D-BEA, the peak at low temperature significantly decreased indicating the removal of the extraframework Al. This result was consistent with the work of Srivastava et al. [17] who employed $^{27}Al$ NMR and $NH_3$-TPD to analyze the removal of extraframework Al from HBEA (Si/Al = 17) by dealumination. The peak at high temperature increased significantly suggesting an increase of hydroxyl nests in the zeolite structure which likely corresponds to vacant sites from the removal of Al from the zeolite framework [9, 10, 20, 21]. From Fe/D-BEA, the peak at high temperature decreased compared to the peak from D-BEA suggesting that Fe was added to the vacant sites. In addition, the hydroxyl nests could be removed thermally during the catalyst calcination [22].

**Fig. 3** $NH_3$-TPD profiles of HBEA, D-BEA and Fe/D-BEA. About 50 mg of each sample was preheated at 500 °C for 1 h in He stream then cooled down to 100 °C, adsorbed with 35 %$NH_3$/He 1 h, purged with He and ramped to 700 °C
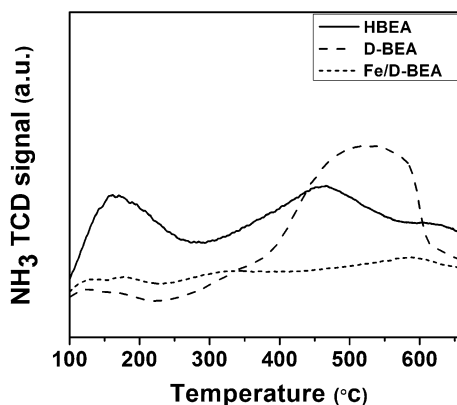
## Catalytic testing of Fe/D-BEA in phenol hydroxylation

Percent phenol conversion and yield from phenol hydroxylation over Fe/D-BEA are shown in Fig. 4a. The conversion 53 % was obtained at 3 min and became steady afterward. The fast reaction was also observed in the previous work on Fe/HBEA [1]. The difference is that the Fe(III) in Fe/HBEA located at the zeolite ion exchange position whereas that in Fe/D-BEA was in the vacant sites generated after dealumination. Fe(III) in both positions had tetrahedral coordination and gave similar phenol conversions. Thus, the different location of Fe(III) with tetrahedral coordination did not lead to different activity in phenol hydroxylation.

Fig. 4b shows the product selectivities from Fe/D-BEA. The major products were catechol (CAT) and hydroquinone (HQ) with mole ratio of 2:1 similar to those from Fe/HBEA [1]. The phenol hydroxylation is known to proceed via the change in oxidation states between Fe(III) and Fe(II) in zeolite framework [23]. The Fe(III) and Fe(II) redox pair generates hydroxyl radical ($^{\cdot}$OH), which attacks at *ortho-* and *para-* positions of phenol to produce CAT and HQ. Moreover, HQ can be oxidized further to benzoquinone (BQ) by excess $H_2O_2$ at the beginning. In this work, a small amount of BQ was detected at 3 min and then disappeared. BQ could be transformed to cokes by a condensation [24]. The formation and disappearance of BQ was also reported by Kullawong et al. [25].

Carbon mass balance from phenol hydroxylation was calculated and the carbon mass loss was defined as "other products". From Fig. 4b, the amount of other products were 20–25 %. In addition, the color of the spent catalyst was dark indicating that cokes were produced. The amount of other products from Fe/D-BEA was less than that in the previous work on Fe/HBEA [1], and thus, the yields of CAT and HQ were higher (see Fig. 5). The lower amount of coke could be attributed to the dealumination of HBEA, which removed Lewis acid sites for the coke formation. The obtained results were in a good agreement with the results from
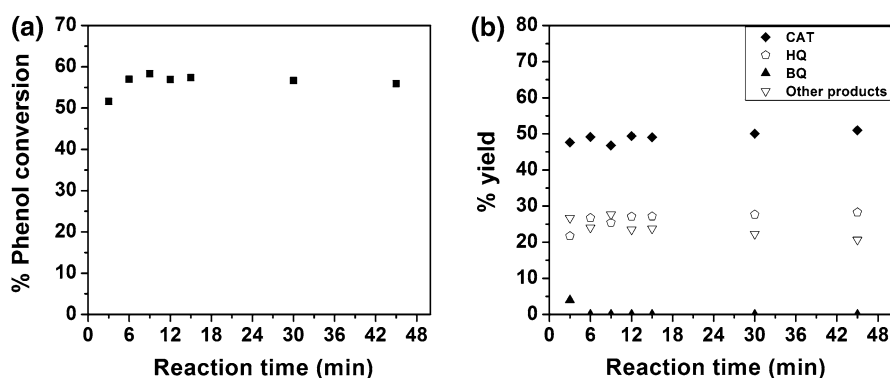


Fig. 4 **a** Percent phenol conversion from phenol hydroxylation and **b** percent catechol yield, percent hydroquinone yield, percent benzoquinone yield and percent other products yield. The Fe/D-BEA catalyst was prepared by stirring D-BEA with a solution of Fe(NO$_3$)$_2$. Reaction conditions: the amount of catalyst = 50 mg, 0.3332 M phenol aqueous solution = 25.0 mL, 30 % $H_2O_2$ = 0.86 mL, the molar ratio of phenol:$H_2O_2$ = 1:1, reaction temperature = 70 °C and stirring speed = 700 rpm
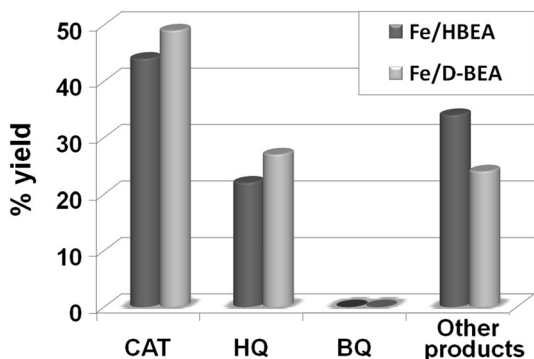
**Fig. 5** Comparing the phenol hydroxylation results between Fe/D-BEA (this work) and Fe/HBEA catalysts (previous work) [1] in terms of percent phenol conversion and product yields. Reaction conditions: the amount of catalyst = 50 mg, 0.3332 M phenol aqueous solution = 25.0 mL, 30 % $H_2O_2$ = 0.86 mL, the molar ratio of phenol:$H_2O_2$ = 1:1, reaction temperature = 70 °C and stirring speed = 700 rpm

Atoguchi et al. [2] in that the higher product yields were obtained from the zeolite with lower aluminum content.

The TPO profiles of the spent Fe/D-BEA and Fe/HBEA are compared in Fig. 6. Cokes on the spent catalysts reacted with oxygen to produced $CO_2$. Thus, the signals of $CO_2$ were proportional to the amounts of cokes. The signals at 250–450 and 450–700 °C corresponded to soft and hard cokes, respectively [26]. The peak area from Fe/D-BEA was smaller than that from Fe/HBEA confirming the less amount of coke. The percent weight loss from Fe/D-BEA to Fe/HBEA were 5.86 and 7.33 %, respectively. These results were consistent with the carbon mass balance. The lower amount of cokes from Fe/D-BEA could be a result from dealumination, which decreased in Lewis acid sites of Fe/D-BEA and probably increased the mass transfer of reactants and products for the reaction [3, 27, 28]. The amount of coke may be reduced further by adding mesopores to the D-BEA. Liu et al. [29] reported that

**Fig. 6** Temperature programmed oxidation (TPO) profiles of spent Fe/D-BEA and Fe/HBEA. About 22 mg of each sample was heated from 25 to 800 °C under 3 % $O_2$ in Ar stream with the flow rate of 20 mL/min
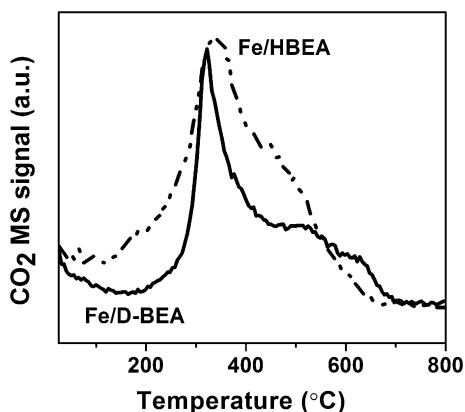
hierarchical BEA with intracrystalline mesoporosity reduced the diffusion length in the zeolite channels and decreases the residence time of methylbenzenes in zeolite micropore. Thus, the better stability against coking than the conventional BEA was achieved.

## Conclusions

Zeolite HBEA was dealuminated by refluxing in nitric acid solution. The obtained D-BEA product was Al-free and showed a slight decrease in the zeolite lattice spacing. The dealumination generated hydroxyl nests or tetrahedral vacant sites which were strongly acidic. The addition of Fe and subsequent calcination suppressed acidity of those sites. The oxidation state of Fe was +3 and it had tetrahedral coordination suggesting the insertion into the vacant sites formerly occupied by Al. From the catalytic testing in phenol hydroxylation, Fe/D-BEA gave a high conversion in 3 min and the maximum conversion 56 % in 6 min. CAT and hydroquinone (HQ) were the major products. However, cokes were still observed after the catalytic testing. Compared to Fe/HBEA in the previous report, the amount of coke from Fe/D-BEA was less and the yields of CAT and HQ from Fe/D-BEA were higher. Thus, a better catalyst for phenol hydroxylation was obtained by loading Fe on dealuminated HBEA.

## References

1. Sophiphun O, Föttinger K, Loiha S, Neramittagapong A, Prayoonpokarach S, Rupprechter G, Wittayakun J (2015) Reac Kinet Mech Cat 116:549–561
2. Atoguchi T, Kanougi T, Yamamoto T, Yao S (2004) J Mol Catal A 220:183–187
3. Corma A (2003) J Catal 216:298–312
4. Borade RB, Clearfield A (1992) J Phys Chem 96:6729–6737
5. Penzien J, Abraham A, van Bokhoven JA, Jentys A, Müller TE, Sievers C, Lercher JA (2004) J Phys Chem B 108:4116–4126
6. Selli E, Rossetti I, Meloni D, Sini F, Forni L (2004) Appl Cat A 262:131–136
7. Tago T, Konna H, Ikeda S, Yamazaki S, Ninomiya W, Nakasaka Y, Masuda T (2011) Catal Today 164:158–162
8. Baran R, Millot Y, Onfroy T, Krafft J-M, Dzwigaj S (2012) Microporous Mesoporous Mater 163:122–130
9. Batonneau-gener I, Yonli A, Hazael-pascal A, Marques JP, Lopes JM, Guisnet M, Ribeiro FR, Mignard S (2008) Microporous Mesoporous Mater 110:480–487
10. Marques JP, Gener I, Ayrault P, Bordado JC, Lopes JM, Ribeiro FR, Guisnet M (2005) C R Chimie 8:399–410
11. Dzwigaj S, Che M (2006) J Phys Chem 110:12490–12493
12. Gurgul J, Łątka K, Hnat I, Rynkowski J, Dzwigaj S (2013) Microporous Mesoporous Mater 168:1–6
13. Čapek L, Kreibich V, Dědeček J, Grygar T, Wichterlová B, Sobalík Z, Martens JA, Brosius R, Tokarová V (2005) Microporous Mesoporous Mater 80:279–289
14. Kumar MS, Schwidder M, Grückner A (2004) J Catal 227:384–397
15. Dzwigaj S, Stievano L, Wagner FE, Che M (2007) J Phys Chem Solids 68:1885–1891

16. Berlier G, Pourny M, Bordiga S, Spoto G, Zecchina A, Lamberti C (2005) J Catal 229:45–54
17. Srivastava R, Iwasa N, Fujita S-I, Arai M (2009) Catal Lett 130:655–663
18. Boroń P, Chmielarz L, Gurgul J, Łątka K, Gil B, Krafft J-M, Dzwigaj S (2014) Catal Today 235:210–225
19. Hegde SG, Kumar R, Bhat RN, Ratnasamy P (1989) Zeolites 9:231–237
20. Wang H, Xin W (2001) Catal Lett 76:225–229
21. Atoguchi T, Kanougi T (2004) J Mol Catal A 222:253–257
22. Senderova E, Halaszb I, Olson DH (2014) Microporous Mesoporous Mater 186:94–100
23. Choi J-S, Yoon S-S, Jang S-H, Ahn W-S (2006) Catal Today 111:280–287
24. Liang X, Yang R, Li G, Hu C (2013) Microporous Mesoporous Mater 182:62–72
25. Kullawong S, Prayoonpokarach S, Neramittagapong A, Wittayakun J (2011) J Ind Eng Chem 17:346–351
26. Guisnet M, Costa L, Ramôa RF (2009) J Mol Catal A 305:69–83
27. Germain G, Allian M, Figueras F (1996) Catal Today 32:145–148
28. Siffert S, Gaillard L, Su B-L (2000) J Mol Catal A 153:267–279
29. Liu Z, Dong X, Zhu Y, Emwas A, Zhang D, Tian Q, Han Y (2015) ACS Catal 5:5837–5845